# Supplementary Information

# Facile preparation of highly sensitive and selective fluorescent paper sensor for the visual and cyclic detection of $Cu^{2+}$ and $Hg^{2+}$

Liying Yu,[a] Yaoyao Qu,[a] Fang Chai[a*] and Lihua Chen[b*]

[a.] Key Laboratory of Photochemical Biomaterials and Energy Storage Materials, Colleges of Heilongjiang Province, College of Chemistry and Chemical Engineering, Harbin Normal University, Harbin, Heilongjiang 150025, China.

E-mail: fangchai@gmail.com

[b.] Shandong Key Laboratory of Biochemical Analysis; College of Chemistry and Molecular Engineering, Qingdao University of Science and Technology, Qingdao 266042, PR China.

E-mail: Lihuachen@qust.edu.cn

The effects of pH on the fluorescence characteristics of the LAA-CQDs were studied in a pH range from 1 to 14. The pH value of the as-prepared of LAA-CQDs was 5. As shown in Figure S1, the fluorescence spectra of LAA-CQDs at different pH values were tested by adjusting amount of buffer solution (potassium acid phthalate, pH=4.08; antipyonin, pH=9.18). The results showed that the pH value increased from 1 to 5 caused the slightly increased of fluorescence intensity, but a further increased from 6.0

to 14.0 led to fluorescence intensity decreased gradually, indicated the fluorescence intensity of LAA-CQDs strongly depended on the pH value.

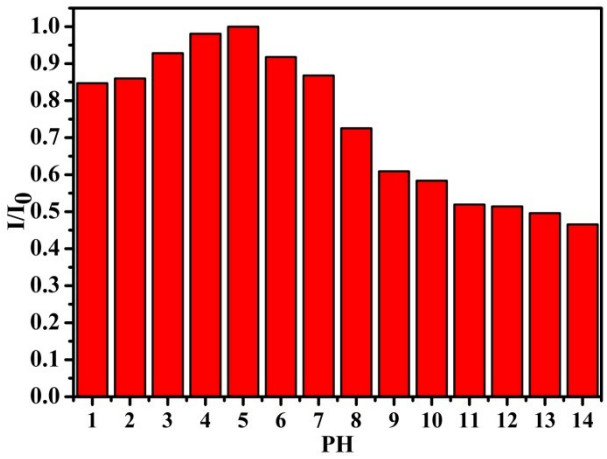


**Figure S1.** The histogram represented the ratio $I/I_0$ of LAA-CQDs under the excitation of 330 nm at different pH condition

Figure S2a and Figure S2b show the time response of fluorescence quenching. As shown in Figure S2a, 2b, the fluorescence intensity decreases quickly and then gets an equilibrium within 60 seconds. So, we choose 60 seconds as the optimal fluorescence quenching time for detection $Cu^{2+}$ and $Hg^{2+}$ (100 μM). Similarly, we choose 5 minutes as the best fluorescence recovering time (Figure S2c, 2d).

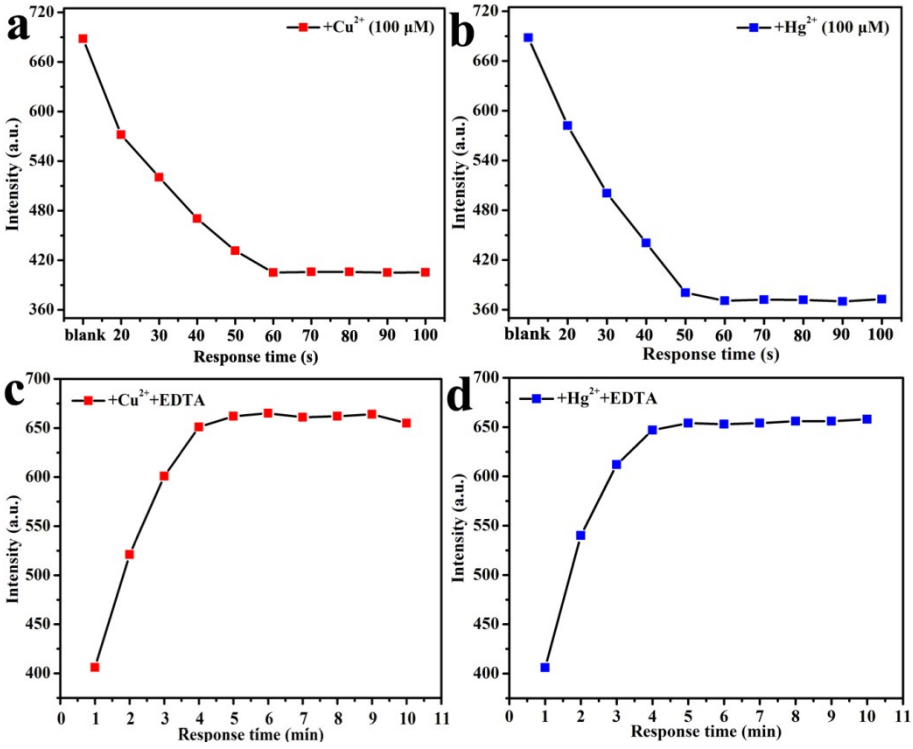


**Figure S2.** Time response of fluorescence quenching ($6.9\times10^{-4}$ mol/L LAA-CQDs and 100 μM (a) $Cu^{2+}$ or (b) $Hg^{2+}$ were mixed in buffer solution and then recorded its fluorescence intensity at different time). Time response of fluorescence recovering (The sample contains $6.9\times10^{-4}$ mol/L LAA-CQDs, 100 μM (c) $Cu^{2+}$ or (d) $Hg^{2+}$ and saturated solution of EDTA, and we recorded its fluorescence intensity at different time).

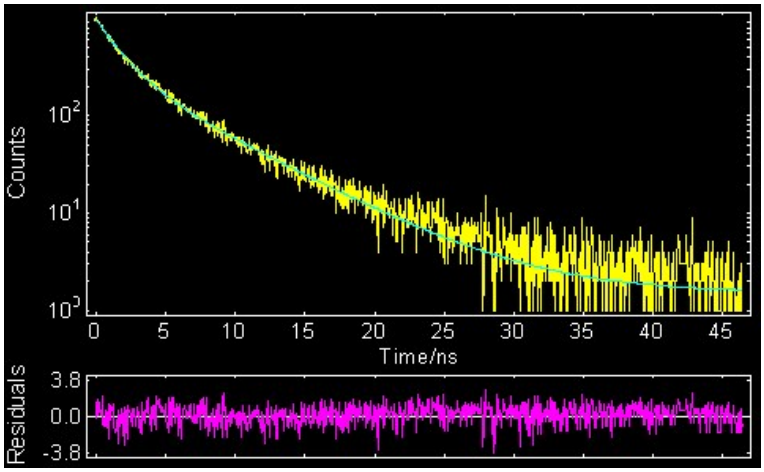


**Figure S3.** Fluorescence decay (yellow lines) and fitting (green lines) curves of LAA-CQDs recorded at emission wavelengths of 410 nm with excitation at 330 nm in ultrapure water.

The fluorescent stability was a significant parameter for an excellent sensor. The fluorescence intensity of LAA-CQDs was recorded for 24 hours without obvious changed in Figure S4.

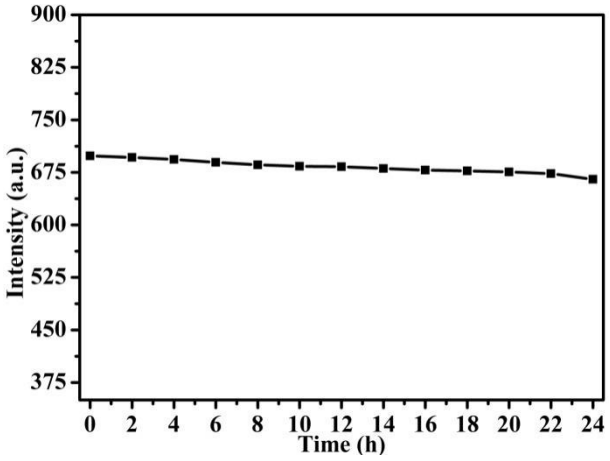


**Figure S4.** The fluorescence intensity of LAA-CQDs recorded each 2 hours for 1 day under 365 nm UV light.

**Selectivity of LAA-CQDs in real water samples**

The selectivity was evaluated as shown in Figure S5, S6, Figure S5a and Figure S6a showed fluorescence spectra of LAA-CQDs containing 100 μM heavy metal ions ($Zn^{2+}$, $Mn^{2+}$, $Fe^{3+}$, $Mg^{2+}$, $Ni^{2+}$, $Co^{2+}$, $Pb^{2+}$, $Cr^{3+}$, $Cr^{6+}$, $Ba^{2+}$, $Cd^{2+}$, $Ca^{2+}$ and $Fe^{2+}$) in tap water and lake water samples compared with $Cu^{2+}$ and $Hg^{2+}$ (100 μM) respectively. The volume ratio of LAA-CQDs and each metal ion was 1: 1. It could be seen that the $Cu^{2+}$ and $Hg^{2+}$ greatly reduced the fluorescence intensity compared with other cations. Relative fluorescence intensity ratio of LAA-CQDs solution containing various heavy metal ions in the tap water and lake water was depicted in Figure S5b and Figure S6b. As described in Figure S5c and Figure S6c, the corresponding photo of detecting multiple ions showed the fluorescence quenching with addition of $Cu^{2+}$ ($Hg^{2+}$) compared with other ions.

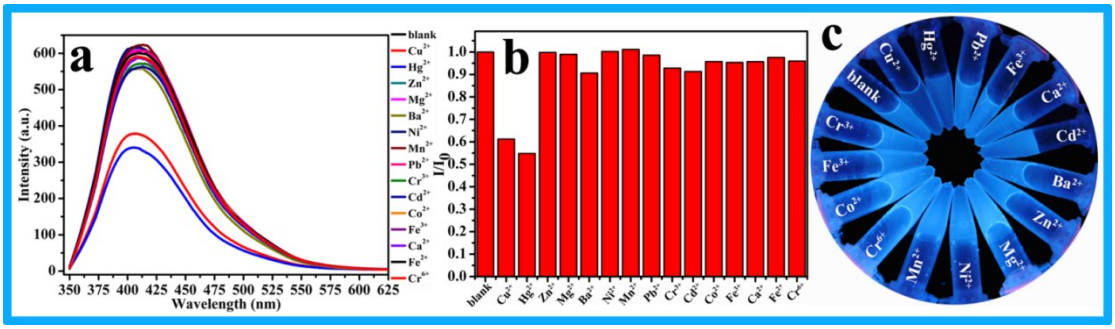


**Figure S5.** Selectivity of ion detection in tap water samples (a) Fluorescence spectrum of LAA-CQDs solutions with adding of a variety of metal ions (100 μM). (b) The relative fluorescence intensity ratio ($\lambda_{ex}$=330 nm) of LAA-CQDs aqueous solution exposed to different ions (100 μM) at 410 nm. (c) The corresponding photograph images of LAA-CQDs exposed to different heavy metal ion samples under UV light (λ=365 nm).

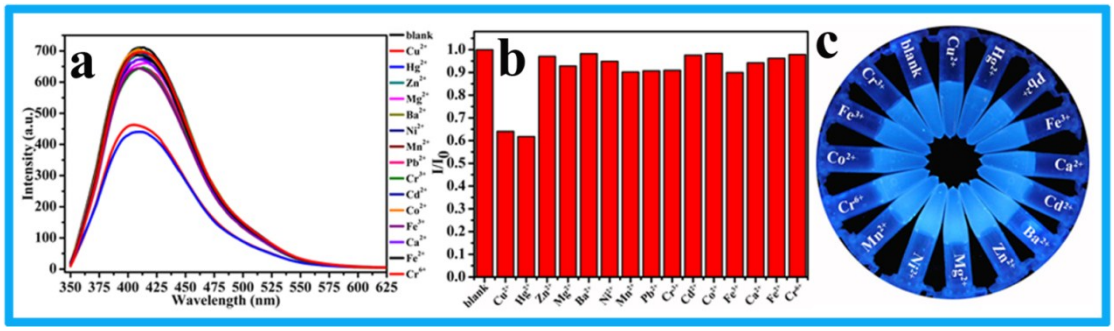


**Figure S6.** Selectivity of ion detection in lake water samples (a) Fluorescence spectrum of LAA-CQDs solutions with adding of a variety of metal ions (100 μM). (b) The relative fluorescence intensity ratio ($\lambda_{ex}$=330 nm) of LAA-CQDs aqueous solution exposed to different ions (100 μM) at 410 nm. (c) The corresponding photograph images of LAA-CQDs exposed to different heavy metal ion samples under UV light (λ=365 nm).

**Sensitivity of LAA-CQDs for $Cu^{2+}$ and $Hg^{2+}$ in tap water**

As shown in Figure S7a, S8a, the emission at 410 nm decreased gradually along with the increase of the concentration of $Cu^{2+}$ ($Hg^{2+}$). The fluorescence intensity ratio and the concentration of $Cu^{2+}$ are linearly related (range from 1 nM to 100 μM) ($I/I_0$=0.954-0.004[$Cu^{2+}$], $R^2$=0.99) (Figure S7b). The liner relationship (range from 0.1 nM to 50 nM) by equation description was that $I/I_0$=0.979-1.084[$Hg^{2+}$], ($R^2$=0.99) (Figure

S8b). The minimum detection limits of $Cu^{2+}$ and $Hg^{2+}$ in tap water were 1.19 μM and 6.15 nM, respectively. The corresponding photo (Figure S7c, S8c) indicated that the fluorescence color gradually changed darker with the increase of concentration of $Cu^{2+}$ ($Hg^{2+}$) under the UV light. In summary, detection of $Cu^{2+}$ ($Hg^{2+}$) by LAA-CQDs in tap water was feasible.

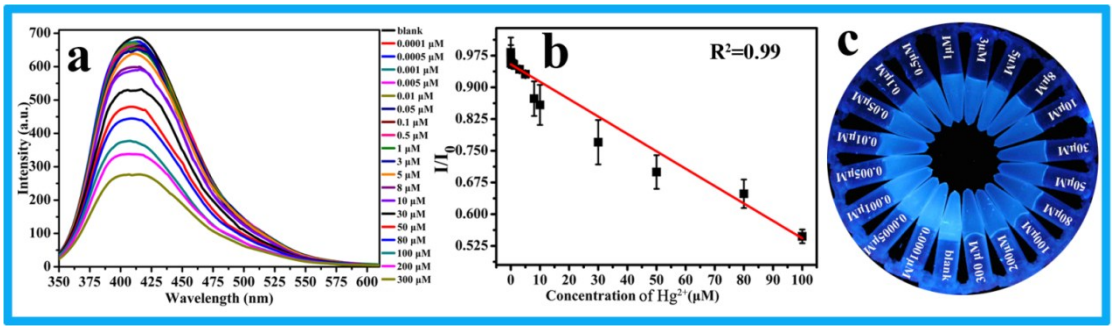


**Figure S7.** (a) Fluorescence spectrum of LAA-CQDs contained different concentrations of $Cu^{2+}$ (0.1 nM-300 μM) under excitation conditions of 330 nm in tap water. (b) The dependence of $I/I_0$ on the concentration of $Cu^{2+}$ ions within the range of 1 nM-100 μM. (c) The corresponding photos of adding $Cu^{2+}$ of different concentrations to the LAA-CQDs solution under UV light (λ=365 nm).

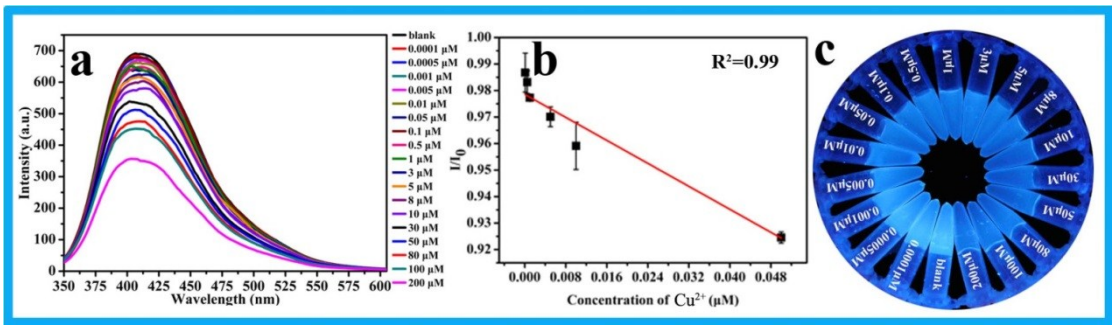


**Figure S8.** (a) Fluorescence spectrum of LAA-CQDs contained different concentrations of $Hg^{2+}$ (0.1 nM-200 μM) under excitation conditions of 330 nm in tap water. (b) The dependence of $I/I_0$ on the concentration of $Hg^{2+}$ within the range of 0.1 nM-50 nM. (c) The corresponding photograph images of adding $Hg^{2+}$ of different concentrations to the LAA-CQDs solution exposed to different concentration of $Hg^{2+}$ ions under UV light (λ=365 nm).

**Sensitivity of LAA-CQDs for $Cu^{2+}$ and $Hg^{2+}$ in lake water**

As descried in Figure S9a, S10a, the remarkable decrease of emission intensity of the LAA-CQDs at 410 nm emerged with the increase of the $Cu^{2+}$ ($Hg^{2+}$) in lake water. As shown in Figure S9b, present a good linear correlation ($I/I_0$=0.927-0.004[$Cu^{2+}$], $R^2$=0.99). And the concentration of the added $Hg^{2+}$ is related to the fluorescence ratio ($I/I_0$=0.954-0.004[$Hg^{2+}$], $R^2$=0.999) (Figure S10b). The calculated results showed the minimum detection limits for the $Cu^{2+}$ and $Hg^{2+}$ in the lake water were 1.35 μM and 1.3 μM, respectively. The change trend of fluorescent color (Figure S9, 10c) under the irradiation of UV lamp was the same as in tap water.

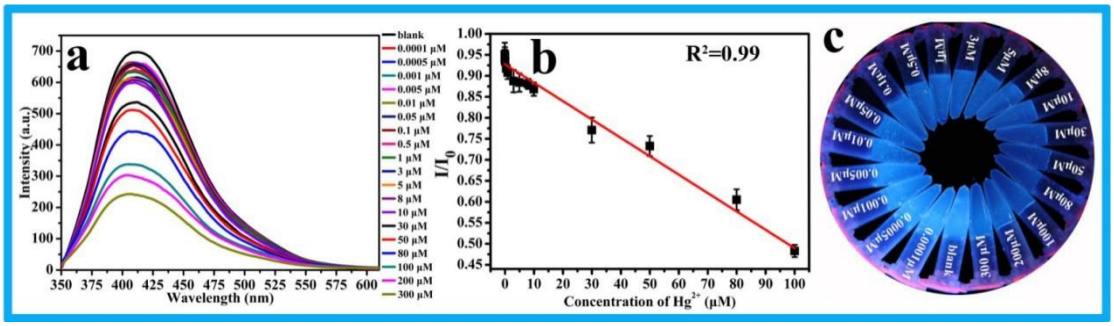


**Figure S9.** (a) Fluorescence spectrum of LAA-CQDs contained different concentrations of $Cu^{2+}$ (0.1 nM-300 μM) under excitation conditions of 330 nm in lake water. (b) The dependence of $I/I_0$ on the concentration of $Cu^{2+}$ ions within the range of 0.5 nM-100 μM. (c) The corresponding photos of adding $Cu^{2+}$ of different concentrations to the LAA-CQDs solution under UV light (λ=365 nm).

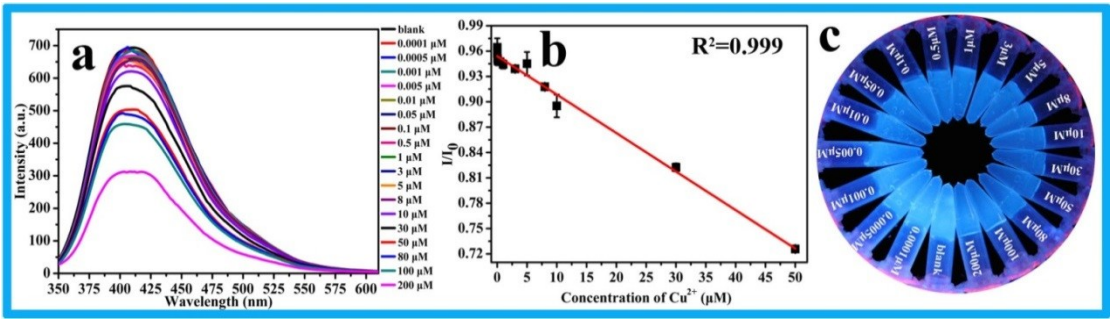


**Figure S10.** (a) Fluorescence spectrum of LAA-CQDs contained different concentrations of $Hg^{2+}$ (0.1 nM-200 μM) under excitation conditions of 330 nm in lake water. (b) The dependence of $I/I_0$ on the concentration of $Hg^{2+}$ within the range of 5 nM-50 μM. (c) The corresponding photograph images of adding $Hg^{2+}$ of different concentrations to the LAA-CQDs solution under UV light (λ=365 nm).

**MTT**

To evaluate the cytotoxicity of the LAA-CQDs, the viability of the HeLa cells was assessed by measuring their ATP activity after exposure to the LAA-CQDs. 100 μL of the cell suspensions in cell media at a concentration of $2\times10^5$ cells/mL were seeded in 96-well plates and allowed to attach overnight. After removal of the cell media, the wells were washed twice with HBSS−HEPES buffer (pH=7.4) and then 100 μL of the tested LAA-CQDs at the relevant concentrations were added. After incubation, the reagent was added to each well to assess the ATP activity.

**Cell Culture and Imaging**

HeLa cells were cultured in Dulbecco's Modified Eagle's Medium supplemented with 10% fetal bovine serum, 100 $mg.mL^{-1}$ penicillin, and 100 $\mu g\cdot mL^{-1}$ streptomycin in a 5% $CO_2$, water saturated incubator at 37 °C and then were seeded in a 12-well culture plate for one night before the cell imaging experiments. For living cell imaging experiments, some of the cells were incubated with 0.019 $g\cdot mL^{-1}$ of probe for 30 min at 37 °C, washed three times with buffer, and then imaged.

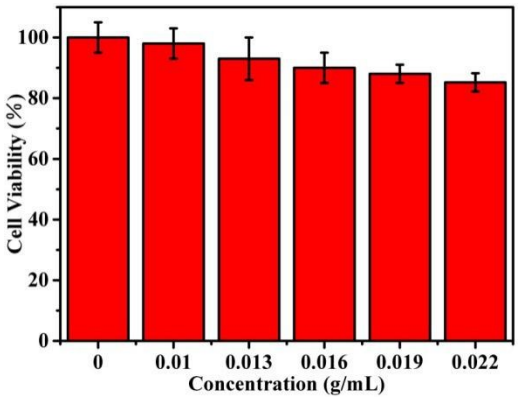


**Figure S11**. Cell viabilities of HeLa cells after incubation with LAA-CQDs for 24 h by MTT assay.

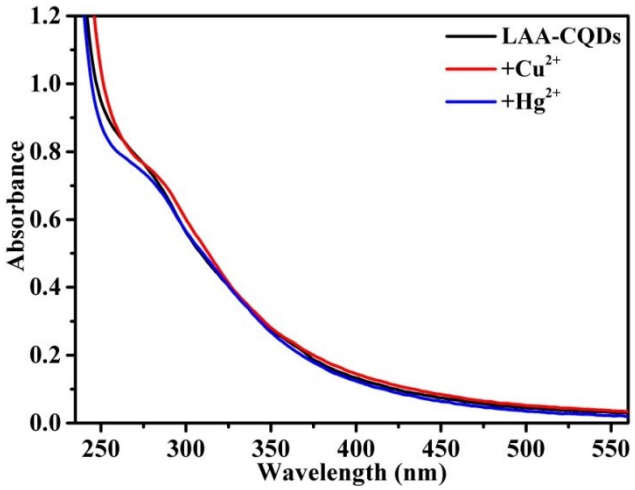


**Figure S12.** Comparison diagram of UV absorption curves of LAA-CQDs, LAA-CQDs+$Cu^{2+}$ and LAA-CQDs+$Hg^{2+}$.

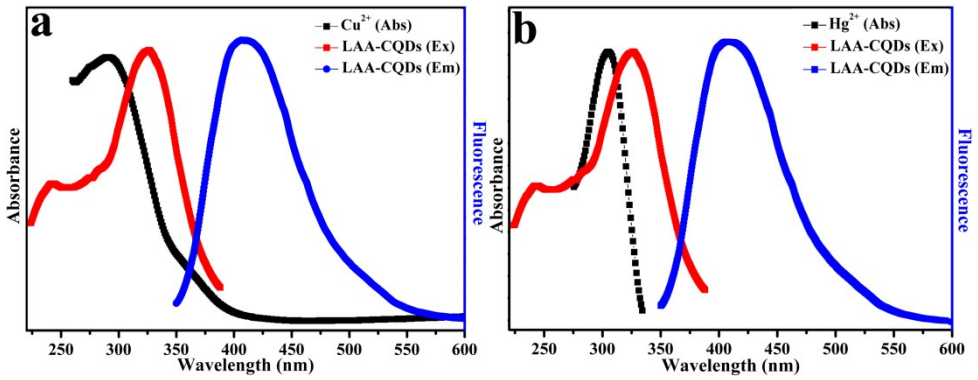


**Figure S13.** The absorption spectrum of black color $Cu^{2+}$ ($Hg^{2+}$), fluorescence excitation spectrum of red color and fluorescence emission spectrum of blue color of LAA-CQDs ($\lambda_{ex}$=330 nm).

**Table S1.** FL lifetimes of LAA-CQDs under excitation at 330 nm

| | Fix | Value / ns | Std. Dev / ns | | Fix | Value | Std. Dev | Rel % |
|---|---|---|---|---|---|---|---|---|
| $\tau_1$ | ☐ | 1.6168 | 0.04708 | $B_1$ | ☐ | 674.146 | 12.2387 | 37.62 |
| $\tau_2$ | ☐ | 5.7841 | 0.09778 | $B_2$ | ☐ | 312.481 | 11.7386 | 62.38 |
| $\tau_3$ | ☐ | | | $B_3$ | ☐ | | | |
| $\tau_4$ | ☐ | | | $B_4$ | ☐ | | | |
| | | | | A | ☐ | 1.520 | | |

$\chi^2$ : 1.095

**Table S2.** Comparison between proposed sensor and previously reported literature values for $Cu^{2+}$ and $Hg^{2+}$ ions detection.

| Systems | Detection Limit | | Detection Method | Reference |
|---|---|---|---|---|
| | $Cu^{2+}$ | $Hg^{2+}$ | | |
| quercetin-Pluronic-F127 nano-micelles | 10 nM | | Fluorescence | [40] |
| pyrene-thiophene conjugate | | 30.6 nM | Fluorescence | [41] |
| Two hexaazatriphenylene-pyrene | | 3.1 nM/12 μM | Fluorescence/paper sensor | [42] |
| carbazole-based probes | 65 nM/ $10^{-5}$ M | | Fluorescence/paper sensor | [43] |
| A phenothiazine-based "naked-eye" fluorescent probe | 97 nM | 80 nM | Fluorescence | [44] |
| Three-dimensional paper-based microfluidic chip device | 35 nM/25 μM | 56 nM/125 μM | Fluorescence/paper sensor | [45] |
| LAA-CQDs | 7.59 nM/5 μM | 2.29 nM/3 μM | Fluorescence/paper sensor | This Work |

**References**


[40] W. N. Jiang, S. L. Yang, W. Lu, B. H. Gao, L. Xu, X. Sun, D. Jiang, H. J. Xu, M. T. Ma and F. L. Cao, *J Photoch Photobio A* 2018, **362**, 14-20.

[41] S. Sarkar, S. Roy, R. N. Saha and S. S. Panja, J*ournal of Fluorescence* 2018, **28**, 427-437.

[42] Y. Li, L. L. Yang, K. Liu, F. Y. Zhao, H. Liu and W. J. Ruan, *New J. Chem.* 2015, **39**, 2429-2432.

[43] L. L. Yang, J. P. Wang, L. Yang, C. Zhang, R. L. Zhang, Z. P. Zhang, B. H. Liu and C. L. Jiang, *RSC Adv.* 2016, **6**, 56384-56391.

[44] M. Kaur, M. J. Cho and D. H. Choi, *Dyes and Pigments* 2016, **125**, 1-7.

[45] J. Qi, B. W. Li, X. R. Wang, Z. Zhang, Z. Wang, J. L. Han and L. L. Chen, *Sensor. Actuat.: B. Chem.* 2017, **251**, 224-233.